SETAC PRESS

Environmental Toxicology and Chemistry, Vol. 28, No. 8, pp. 1592–1598, 2009

Printed in the USA
0730-7268/09 $12.00 + .00

IMPACT OF KEROGEN HETEROGENEITY ON SORPTION OF ORGANIC POLLUTANTS. 2. SORPTION EQUILIBRIA

CHEN YANG,† ZHIQIANG YU,‡ BAOHUA XIAO,§ WEILIN HUANG,*‖ JIAMO FU,‡ and ZHI DANG†
†School of Environmental Science and Engineering, South China University of Technology, University Town, Guangzhou 510006, China
‡State Key Laboratory of Organic Geochemistry, Guangzhou Institute of Geochemistry, Chinese Academy of Sciences, Wushan, Guangzhou 510640, China
§State Key Laboratory of Environmental Geochemistry, Institute of Geochemistry, Chinese Academy of Sciences, Guiyang, Guizhou Province, 550002, China
‖Department of Environmental Sciences, Rutgers University, New Brunswick, New Jersey 08901-8551, USA

(*Received* 30 *October* 2008; *Accepted* 2 *March* 2009)

Abstract—Phenanthrene and naphthalene sorption isotherms were measured for three different series of kerogen materials using completely mixed batch reactors. Sorption isotherms were nonlinear for each sorbate–sorbent system, and the Freundlich isotherm equation fit the sorption data well. The Freundlich isotherm linearity parameter n ranged from 0.192 to 0.729 for phenanthrene and from 0.389 to 0.731 for naphthalene. The n values correlated linearly with rigidity and aromaticity of the kerogen matrix, but the single-point, organic carbon–normalized distribution coefficients varied dramatically among the tested sorbents. A dual-mode sorption equation consisting of a linear partitioning domain and a Langmuir adsorption domain adequately quantified the overall sorption equilibrium for each sorbent–sorbate system. Both models fit the data well, with r^2 values of 0.965 to 0.996 for the Freundlich model and 0.963 to 0.997 for the dual-mode model for the phenanthrene sorption isotherms. The dual-mode model fitting results showed that as the rigidity and aromaticity of the kerogen matrix increased, the contribution of the linear partitioning domain to the overall sorption equilibrium decreased, whereas the contribution of the Langmuir adsorption domain increased. The present study suggested that kerogen materials found in soils and sediments should not be treated as a single, unified, carbonaceous sorbent phase.

Keywords—Kerogen Black carbon Phenanthrene Naphthalene Sorption isotherm

INTRODUCTION

Kerogen-containing particles, such as coal and charcoal, are commonly found in soils and sediments [1–3]. Their roles in sorption and sequestration of hydrophobic organic contaminants (HOCs) in aquatic systems have been delineated in great detail over the past 15 years [4,5]. Kerogen particles are very strong sorbents for HOCs, such as polynuclear aromatic hydrocarbons (PAHs) and polychlorinated biphenyls [6–8]. They are the dominant sorbents and they dominate the nonlinear sorption isotherms [9,10]. The rates of HOC sorption on these particles are extremely slow, and subsequent desorption rates are even slower, resulting in a significant apparent hysteretic phenomenon [5,11]. They also are responsible for strong, competitive sorption among multiple HOC solutes [12]. These phenomena could not be interpreted readily with the well-known partitioning theory [13].

A recent study by Song et al. [1] showed that matured kerogen and black carbon or soot particles are important organic constituents in soils and sediments of industrial areas and that their contents vary from a few percent to as high as 80% of the total organic carbon. Xiao et al. [10] found that the phenanthrene sorption isotherms measured for the same set of soils and sediments studied by Song et al. [1] were variously nonlinear, with Freundlich isotherm n parameter values ranging from 0.469 to 0.784 for phenanthrene and from 0.416 to 0.792 for naphthalene. Their measured organic carbon–normalized sorption distribution coefficient (K_{OC}) ranged from 3.83 to 7.19×10^4 L/kg at an aqueous phase phenanthrene concentration of 0.0056 mg/L, compared to 1 to 2×10^4 L/kg predicted from the log K_{OC}/log octanol–water partition coefficient (K_{OW}) correlations based on the well-known linear partition model [14].

Cornelissen et al. [4] summarized the sorption properties for a wide range of carbonaceous geosorbents (CGs). Those authors found that the contribution of CGs to the overall sorption of a given HOC on sediments may vary over a wide range, because CGs may have very different physicochemical properties. As shown in the first paper of this series [15], kerogen materials that originate from different source materials have very different physicochemical properties, and the kerogens of the same source material possess a wide range of compositional as well as structural and physical properties because of differences in thermal or diagenetical histories. This heterogeneous nature should have a strong impact on both the equilibria and rates of HOC sorption from aqueous solutions.

The goal of the present study was to demonstrate a diverse spectrum of equilibrium sorption reactivities for chemically and structurally heterogeneous kerogen particles. In the present study, the kerogen samples prepared and characterized in the first paper [15] were used as the sorbents. The objectives were to measure the equilibrium sorption isotherm for the kerogen materials, to correlate the sorption isotherm parameters and sorption distribution coefficients with the chemical and structural properties of the sorbents, and to elucidate the mechanisms for the observed sorption phenomena.

* To whom correspondence may be addressed (whuang@envsci.rutgers.edu).
Published on the Web 3/23/2009.

MATERIALS AND METHODS

Chemicals and solutions

Phenanthrene and naphthalene (high-performance liquid chromatography [HPLC] grade; Aldrich Chemical) were used as the sorbates, because their sorption properties have been examined extensively in previous studies [16–18]. The log K_{OW} values of phenanthrene and naphthalene are 4.57 and 3.30, respectively, and their aqueous solubilities (S_W) at 20°C are approximately 1.12 and 31.5 mg/L, respectively. Organic solvents, methanol and acetonitrile (HPLC grade; Fisher Scientific), and $CaCl_2$, NaN_3, and $NaHCO_3$ (Aldrich Chemical) were used as received.

The aqueous solution used in the sorption experiments contained 0.005 mol/L of $CaCl_2$ as the major mineral constituent, 100 mg/L of NaN_3 for inhibiting microorganism growth, and 5 mg/L of $NaHCO_3$ to buffer the solution at pH 7.0. The primary stock solutions of phenanthrene and naphthalene and their initial aqueous solutions were prepared as described previously [19]. All the stock methanol solutions were stored at −4°C in vials sealed with Teflon®-lined tops. The initial aqueous solutions (C_0) were prepared by mixing a given volume of an appropriate stock solution with background aqueous solution in a volumetric flask. Methanol concentrations in the initial aqueous solutions were below 0.2% by volume, the level at or below which the effect of methanol on sorption is insignificant [20].

Sorbents

Three series of kerogen materials (coals; particle size, 63–100 μm) were employed as the sorbents in the present study: Lopinite (LP) series (five samples), originally from Mingshan Coal Mine (Leping, Jiangxi Province, China) and consisting of type II kerogen with suberinite (or barkinite) as the dominant organic matrix, which is derived from the bark tissue of woody plants and is identified as suberinized cell walls in cork tissue, with cell cavities usually filled by secondary gelification materials; lignite (XF) series (eight samples), originally from Xianfeng Coal Mine (Kunming, Yunnan Province, China) and containing type III kerogen with vitrinite as the dominant organic matrix, which is a major maceral of coal materials of relatively higher grades derived diagenetically from plant or humic materials and is identified with characteristics of gray color and smooth, homogeneous surfaces; and fusinite (HZ) series (five samples), originally from Haizhou Coal Mine (Fuxing, Liaoning Province, China) and consisting of type IV kerogen with fusinite as the dominant organic matrix, which has unique burning and charring properties and is characterized by its brightness, irregular dark-colored pores, and well-preserved cellular structures. As described in the first paper of this series [15], each series was prepared with a thermal treatment procedure at temperature ranging from 200 to 500°C to simulate diagenesis and catagenesis of kerogen. The kerogen materials of a given series have identical source material but different simulated diagenetical histories. The treated samples of each series were labeled from 1 to 7 (e.g., XF1), corresponding to the treatment temperatures from 200 to 500°C. The pretreatment process and the physicochemical properties of sorbents were characterized and presented in the first paper of this series [15].

Sorption experiments

Sorption experiments were conducted at room temperature (22 ± 0.5°C, mean ± range) using flame-sealed glass ampoules (20 and 50 ml; VWR) as the completely mixed batch reactor (CMBR) systems. The detailed procedures have been described previously [19,21]. For all the sorbent–sorbate systems examined, preliminary tests were conducted to determine both the time (42 d) required for attaining apparent sorption equilibrium and the appropriate solid to solution ratios for achieving 30 to 70% reduction of the initial aqueous-phase concentrations. The contact time used might not be sufficiently long for attaining true sorption equilibrium. Final sorption experiments were conducted to acquire the equilibrium data reported here. Each CMBR contained an appropriate sorbent mass and initial aqueous solution, with a headspace of approximately 0.8 ml. The CMBRs were packed in boxes placed on a shaker (Orbital; VWR) set at 125 rpm. They also were mixed from top to bottom, by hand, several times a week, with each mixing lasting for several minutes. After 42 d of mixing, the ampoules were set upright for 2 d to allow the sorbent particles to settle. Ampoules were then opened, and an aliquot (3 ml) of the supernatant was immediately withdrawn from each and mixed with 1.5 ml of methanol in a 5-ml glass vial (VWR). The amounts of methanol and aqueous solution were weighed, and a dilution factor was calculated based on mass ratio and the density data of the mixture [22]. The mixture was analyzed for the sorbate concentration with HPLC. The equilibrium aqueous-phase concentration of the sorbate (C_e) was calculated from the HPLC result and the dilution factor.

Control experiments were conducted similarly, using ampoules free of sorbents for assessing loss of solutes during tests. The results showed that the average system losses were consistently less than 4% of initial aqueous-phase concentrations for the two sorbates. Hence, no correction was made during reduction of final sorption data.

HPLC analysis

Both C_0 and C_e of the two sorbates were measured using reverse-phase HPLC (Agilent Model 1100) with an ODS column (length, 250 mm; inner diameter, 2.1 mm; film thickness, 5 μm). The instrument had a diode-array ultraviolet detector (wavelength set at 250 nm for phenanthrene and 220 nm for naphthalene) and a fluorescence detector (ultraviolet excitation/emission wavelengths at 250/332 nm for phenanthrene and 250/364 nm for naphthalene). The mobile phase used was a mixture of acetonitrile and water at a volumetric ratio of 90:10 for phenanthrene and 88:12 for naphthalene. External standards of phenanthrene (0.5–1,000 μg/L) and naphthalene (6–20,000 μg/L) in methanol matrix were used to establish linear calibration curves. The equilibrium solid-phase sorbate concentrations (q_e) were computed based on the mass balance of the solute between the two phases.

Modeling

The equilibrium sorption data obtained for the two sorbates and the 18 sorbents were fit to the Freundlich sorption model having the following form:

$$\log q_e = \log K_F + n \log C_e$$

where K_F ((mg/kg)/(mg/L)^n) and n are the Freundlich sorption coefficient and the isotherm nonlinearity index, respectively, and q_e (mg/kg) and C_e (mg/L) are as defined above. Statistics software (Systat, Ver 10.0; Systat Software) was used to compute both Freundlich model parameters with standard deviations. The resulting log K_F and n values, along with their standard deviations and r^2 values, are summarized in Table 1.

Table 1. List of Freundlich isotherm parameters for the lignite (XF) series, lopinite (LP) series, and fusinite (HZ) series samples[a]

	Phenanthrene						Naphthalene					
				log K_{OC}[c] at C_e/S_W =						log K_{OC}[c] at C_e/S_W =		
Sample	log K_F[b]	n	r^2	0.005	0.05	0.5	log K_F[b]	n	r^2	0.005	0.05	0.5
XF0	4.555 ± 0.014	0.650 ± 0.010	0.996	5.56	5.21	4.86	3.601 ± 0.009	0.731 ± 0.010	0.997	4.04	3.77	3.50
XF1	4.705 ± 0.014	0.637 ± 0.010	0.995	5.73	5.36	5.00	3.754 ± 0.007	0.702 ± 0.008	0.998	4.20	3.90	3.60
XF2	4.783 ± 0.015	0.629 ± 0.011	0.995	5.81	5.44	5.07	—	—	—	—	—	—
XF3	4.828 ± 0.012	0.577 ± 0.008	0.996	5.96	5.54	5.12	4.104 ± 0.009	0.625 ± 0.010	0.996	4.59	4.21	3.84
XF4	4.712 ± 0.015	0.492 ± 0.009	0.994	6.01	5.50	5.00	—	—	—	—	—	—
XF5	4.013 ± 0.020	0.391 ± 0.012	0.986	5.51	4.90	4.29	3.883 ± 0.011	0.489 ± 0.011	0.99	4.42	3.91	3.40
XF6	3.547 ± 0.015	0.304 ± 0.009	0.986	5.22	4.53	3.83	—	—	—	—	—	—
XF7	3.487 ± 0.011	0.242 ± 0.008	0.986	5.29	4.53	3.77	3.819 ± 0.023	0.406 ± 0.025	0.938	4.39	3.79	3.20
LP0	3.930 ± 0.012	0.562 ± 0.012	0.993	5.03	4.60	4.16	3.797 ± 0.009	0.508 ± 0.009	0.995	4.31	3.82	3.33
LP1	4.105 ± 0.014	0.596 ± 0.014	0.992	5.13	4.73	4.32	3.897 ± 0.008	0.558 ± 0.007	0.997	4.37	3.93	3.48
LP3	4.249 ± 0.020	0.729 ± 0.018	0.991	4.97	4.70	4.43	4.105 ± 0.011	0.613 ± 0.010	0.995	4.53	4.14	3.76
LP5	3.481 ± 0.011	0.429 ± 0.010	0.991	4.87	4.30	3.73	3.245 ± 0.008	0.469 ± 0.008	0.994	3.77	3.24	2.71
LP7	2.955 ± 0.013	0.299 ± 0.012	0.974	4.63	3.93	3.23	3.013 ± 0.009	0.412 ± 0.009	0.991	3.58	2.99	2.40
HZ0	4.794 ± 0.013	0.570 ± 0.011	0.992	5.89	5.46	5.03	4.243 ± 0.005	0.505 ± 0.006	0.998	4.77	4.27	3.78
HZ1	4.735 ± 0.013	0.549 ± 0.011	0.992	5.88	5.42	4.97	4.250 ± 0.010	0.502 ± 0.010	0.993	4.77	4.28	3.78
HZ3	4.747 ± 0.019	0.591 ± 0.015	0.989	5.79	5.38	4.97	4.277 ± 0.008	0.500 ± 0.009	0.994	4.80	4.30	3.80
HZ5	3.702 ± 0.009	0.402 ± 0.008	0.992	5.14	4.54	3.94	3.790 ± 0.015	0.460 ± 0.016	0.979	4.31	3.77	3.23
HZ7	3.929 ± 0.010	0.192 ± 0.009	0.965	5.82	5.02	4.21	4.222 ± 0.022	0.389 ± 0.022	0.945	4.79	4.18	3.57

[a] C_e = equilibrium aqueous-phase concentration of the sorbate; K_F = Freundlich sorption coefficient; K_{OC} = organic carbon–normalized sorption distribution coefficient; n = isotherm nonlinearity index; SW = aqueous solubility; — = not measured.
[b] Units in (mg/kg)/(mg/L)^n.
[c] Units in (L/kg), calculated using the Freundlich isotherm parameters and the organic carbon contents.

The single-point K_{OC} values (equal to (q_e/C_e)/mass fraction of organic carbon [f_{OC}] calculated at specific C_e levels for both phenanthrene and naphthalene are also listed in Table 1.

To illustrate the sorption mechanism, we fit the sorption data to a simplified, dual-mode sorption model having the following form [23]:

$$q_e = K_{D,L}C_e + \frac{Q_a^\circ bC_e}{1 + bC_e}$$

where $K_{D,L}$ (L/kg) is the distribution or partitioning coefficient for the aliphatic domain and b (L/mg) and Q_a° (mg/kg) are the Langmuir site energy and capacity factor for the aromatic domain, respectively. The statistical data resulting from using the same software are summarized in Table 2, and the model fittings to the experimental data are shown in *Supporting Information,* Figures S1 and S2 (http://dx.doi.org/10.1897/08-550.S1).

RESULTS AND DISCUSSION

Sorption isotherms

As shown in Table 1 and Figure 1, the Freundlich isotherm model fits the equilibrium sorption data well, with r^2 values ranging from 0.965 to 0.996 for phenanthrene and from 0.938 to 0.998 for naphthalene. All 18 sorption isotherms are nonlinear, with n values ranging from 0.192 to 0.729 for phenanthrene and from 0.389 to 0.731 for naphthalene, which is consistent with previous reports [10,16]. From Table 1, it also could be observed that for a given sorbent, the phenanthrene sorption isotherm was more nonlinear than naphthalene, likely because of the larger molecular size and greater hydrophobicity of phenanthrene. For a given sorbate, the n values varied among the three different series of kerogen materials. For the XF series, the n values of the phenanthrene isotherms decreased as the maturation increased, from 0.650 for XF0 to 0.242 for XF7. For the LP series, the n values of the phenanthrene isotherms increased initially from 0.562 for LP0 to 0.729 for LP3 and then decreased to 0.299 for LP7. For the HZ series, the n values of the phenanthrene isotherms stayed relatively constant, between 0.549 to 0.591, for HZ0 to HZ3 and then decreased to 0.192 for HZ7. Similar trends could be observed for the naphthalene sorption isotherms.

As shown in Table 1, the log K_F values measured for all the sorbents varied from 2.955 to 4.828 for phenanthrene and from 3.013 to 4.277 for naphthalene. This is consistent with a report of phenanthrene sorption on coal materials [16]. To better illustrate the relationship between sorption capacity

Table 2. List of dual-mode model parameters for the lignite (XF) series, lopinite (LP) series and fusinite (HZ) series samples[a]

Sample	$K_{D,L}$ (L/kg)	Q_a° (mg/kg)	b (L/mg)	r^2
Phenanthrene				
LP0	5,343 ± 811	3,547 ± 676	12.0 ± 4.08	0.986
XF3	42,165 ± 3,790	25,780 ± 3,205	13.9 ± 3.38	0.993
HZ0	29,603 ± 3,099	30,857 ± 2,964	10.4 ± 1.83	0.994
LP5	1,375 ± 158	1,609 ± 101	21.7 ± 3.00	0.992
XF5	6,502 ± 826	4,242 ± 333	66.8 ± 13.6	0.987
HZ5	2,606 ± 142	2,535 ± 85.4	29.7 ± 2.47	0.997
LP7	182 ± 62.1	653 ± 39.4	30.1 ± 4.73	0.973
XF7	2,817 ± 216	1,400 ± 67.2	293 ± 72.2	0.977
HZ7	2,054 ± 407	6,283 ± 223	87.4 ± 12.3	0.963
Naphthalene				
LP0	2,733 ± 132	3,432 ± 234	11.9 ± 1.98	0.995
XF3	2,887 ± 379	22,393 ± 4,113	1.02 ± 0.35	0.994
HZ0	3,259 ± 280	24,315 ± 2,397	1.89 ± 0.41	0.993
LP5	205 ± 47.8	2,518 ± 261	2.36 ± 0.49	0.988
XF5	956 ± 123	11,589 ± 952	2.07 ± 0.38	0.992
HZ5	516 ± 116	9,736 ± 847	2.23 ± 0.43	0.987
LP7	129 ± 31.8	1,195 ± 117	4.33 ± 0.98	0.978
XF7	693 ± 95.1	7,541 ± 442	6.22 ± 0.99	0.983
HZ7	2,124 ± 256	16,872 ± 912	8.66 ± 1.28	0.986

[a] b = capacity factor for the aromatic domain; $K_{D,L}$ = distribution or partitioning coefficient for the aliphatic domain; b (L/mg) and Q_a° = Langmuir site energy.

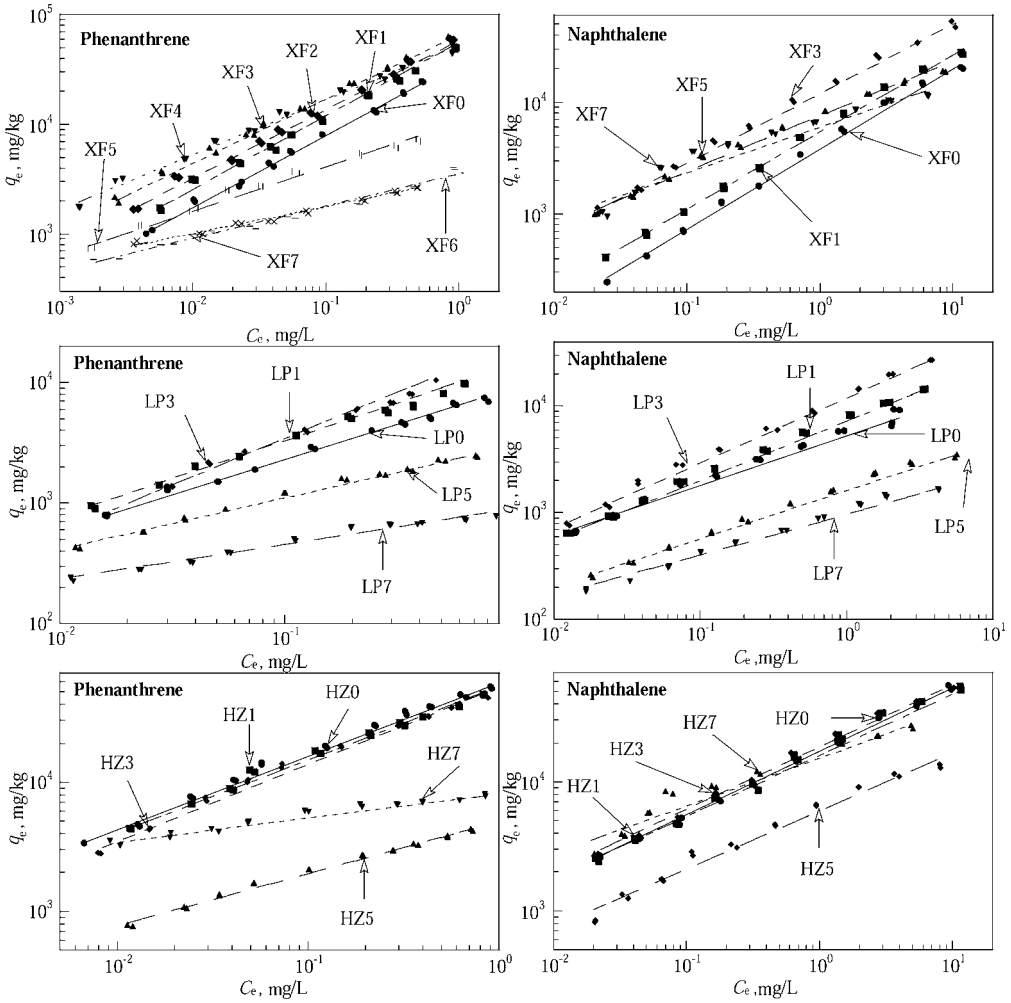

Fig. 1. Sorption isotherms measured for the lopinite (LP) series, lignite (XF) series, and fusinite (HZ) series.

properties and the sorbent properties, single-point K_{OC} values at C_e/S_W = 0.005, 0.05, and 0.5 were calculated from the same set of the sorption isotherm parameters. The log K_{OC} values listed in Table 1 indicate that because of its greater hydrophobicity, phenanthrene has much greater sorption capacity than naphthalene on the same sorbent, and that sorption capacity for a single sorbent–solute system decreased sharply as a function of C_e, mainly because of the effect of isotherm nonlinearity. It was shown in Table 1 that the log K_{OC} values calculated for a given solute varied dramatically among different sorbents. For the XF series, the phenanthrene log K_{OC} values calculated at C_e/S_W = 0.005 increased from 5.56 for XF0 to 6.01 for XF4 and then decreased to 5.29 for XF7. For the LP series, the phenanthrene log K_{OC} values calculated at C_e/S_W = 0.005 increased from 5.03 for LP0 to 5.13 for LP1 and then decreased to 4.63 for LP7. For the HZ samples, values decreased from 5.89 for HZ0 to 5.14 for HZ5 and then increased to 5.82 for HZ7. Similar trends could be found for phenanthrene at C_e/S_W =0.05 and 0.5 and for naphthalene at C_e/S_W = 0.005, 0.05, and 0.5. These results are consisted with the literature data (4.6–6.9 L/kg) reported previously [4] for BC, coal, and kerogen.

Impacts of kerogen properties

The equilibrium sorption properties delineated above appear to depend strongly on the maturation and the parental sources of the kerogen materials. Figure 2 shows that the sorption isotherm linearity (n) correlates inversely with the reflectance index ($R°$) and aromaticity (f_a) of the sorbents and positively with the atomic ratios of oxygen to carbon and of hydrogen to carbon. These linear correlations strongly suggested that a physically more condensed, chemically more reduced, and structurally more aromatic organic matrix exhibits greater isotherm nonlinearity. This observation is consistent with those in previous studies [16,18,21]. Cornelissen and Gustafsson [16] reported that the sorption nonlinearity for five medium-ranked coals correlates with their total organic carbon content as the total organic carbon increases as a function of coal maturation. Xing [18] had reported that the phenanthrene and naphthalene Freundlich exponent n values correlated inversely with the aromaticity of humic acids. Huang and Weber [21] also reported that the sorption isotherm nonlinearities for phenanthrene correlated inversely with the oxygen to carbon (O/C) atomic ratio of sediment organic matter. Those authors reported a regression equation of n = 0.409 + 0.704(O/C), with r^2 = 0.911.

The sorption capacities represented by the single-point K_{OC} values (Table 1) vary dramatically among the 18 sorbents and are inconsistent with the observations reported by Huang and Weber [21]. Those authors examined equilibrium sorption of phenanthrene on soil and sediment samples having a wide range of diagenetical histories. They found that the single-

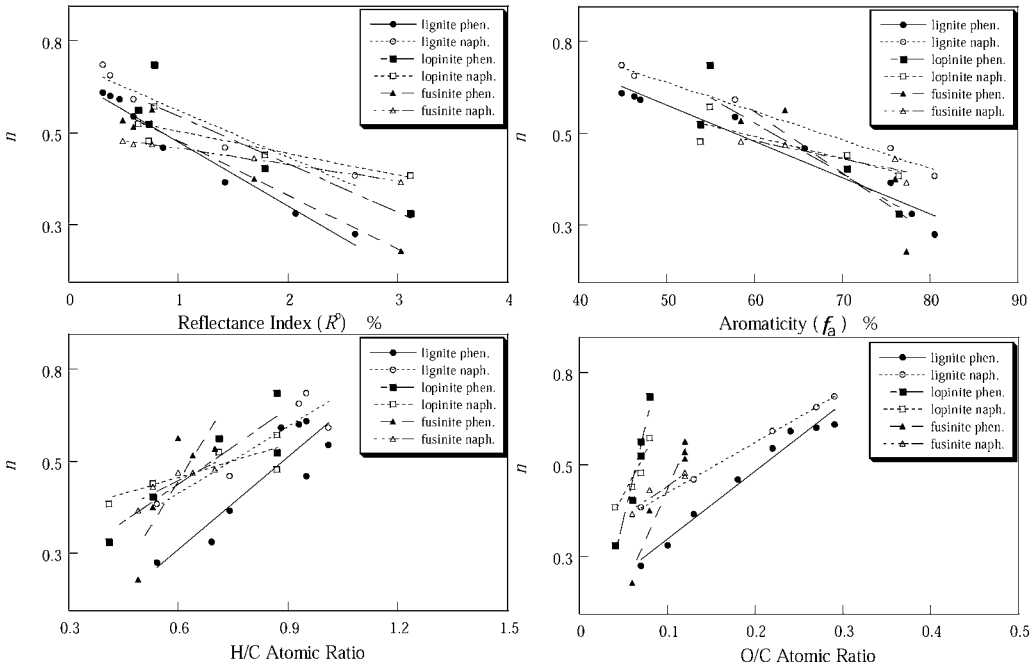

Fig. 2. The correlations among reflectance index of vitrinite ($R°$), aromaticity (f_a), hydrogen to carbon (H/C) and oxygen to carbon (O/C) atomic ratios, and the isotherm nonlinearity. naph. = naphthalene; phen. = phenanthrene.

point phenanthrene K_{OC} value at a given C_e decreases as a function of the O/C atomic ratio of soil/sediment organic matter—that is, log K_{OC} = 4.39–4.63(O/C) at C_e = 1 μg/L, r^2 = 0.918, and log K_{OC} = 2.62–2.54(O/C) at C_e = 1,000 μg/L, r^2 = 0.826. Such linear relationships were only consistent with our observations for the less matured samples (i.e., XF0 to XF3, LP0 and LP1, and HZ0 and HZ1). As the oxgen to carbon atomic ratio of kerogen matrix decreases as a function of maturation, the single-point K_{OC} value increases initially, reaches the maximum value at approximately 300°C, and then decreases. It was likely that the samples selected in the literature were possibly less matured, and that the observed sorption phenomena may not be representative of the kerogen that has undergone more severe alterations.

Possible sorption mechanisms

The observed variations in equilibrium sorption of the two chemicals can be explained in terms of structural heterogeneity of the kerogen matrix. As noted in the organic geochemistry literature [24,25], kerogen matrices consisted mainly of two organic domains, a structurally flexible aliphatic domain and a physically rigid aromatic domain with strong C=C or C=O=C bridges or cross-linkages. The relative contents of the two structurally different organic domains depended on the type and maturity of the kerogen. For a specific type or series of kerogen samples, the content of the aliphatic domain decreases, and that of the aromatic domain increases, as a function of the degree of maturation of the organic matrix during diagenesis [26]. Such changes are strongly supported by the physical, chemical, and spectroscopic properties, such as elemental compositions, ^{13}C nuclear magnetic resonance, and Fourier transform infrared spectra reported in the first paper of this series [15].

It is expected that the sorption of phenanthrene and naphthalene is very different within the two organic domains of the kerogen matrix. Sorption into the structurally flexible aliphatic domain may likely follow an absorption or partitioning process with a relatively linear relationship between the sorbate concentration within the domain and C_e. Sorption into the structurally rigid aromatic domain may be dominated by adsorption of the sorbate molecules at the internal and external surfaces of the domain; resulting in a capacity-limited, nonlinear relationship between the sorbate concentration within the domain and C_e.

For a given kerogen series, the calculated contribution of linear partitioning to the overall sorption of both phenanthrene and naphthalene generally decreases as the kerogen maturation increases, whereas the calculated contributino of nonlinear adsorption increases accordingly, as evidenced in the *Supporting Information,* Figures S1 and S2 (http://dx.doi.org/10.1897/08-550.S1). Among the three series of kerogen materials and for a given maturation, the XF series exhibited greater contribution of the linear component, whereas the HZ series exhibited more contribution of the nonlinear adsorption component. For the convenience of further discussion, we chose the XF3, XF5, and XF7 samples from the XF series; the LP0, LP5, and LP7 samples from the LP series; and the HZ0, HZ5, and HZ7 samples from the HZ series, representing low (XF3, LP0, and HZ0; $R° < 0.6\%$), medium (XF5, LP5, and HZ5; $R°$ = 1.4–1.7%), and high (XF7, LP7, and HZ7; $R° > 2.5\%$) maturation. According to Table 2, the $K_{D,L}$ values calculated for phenanthrene decrease from 5,343, 42,165, and 29,603 L/kg for LP0, XF3, and HZ0, respectively, to 182, 2,817, and 2,054 L/kg for LP7, XF7, and HZ7, respectively. The Q_a° value decreases from 3,547 and 25,780 mg/kg for LP0 and XF3, respectively, to 653 and 1,400 mg/kg for LP7 and XF7, respectively. It should be noted that the Q_a° value calculated for HZ samples has a different trend—that is, decreasing from 30,857 mg/kg (HZ0) to 4,242 mg/kg (HZ5), and then increasing to 6,283 mg/kg (HZ7). The parameter *b* for the XF samples increases dramatically, from 13.9 L/mg (XF3) to 293 L/mg (XF7), whereas the *b* value for both LP and HZ samples increases gradually, from 12.0 L/mg (LP0) and 10.4 L/mg (HZ0)

to 30.1 L/mg (LP7) and 87.4 L/mg (HZ7). Similar trends also were observed for naphthalene.

We can conclude from the results and discussion in the first paper of this series [15] that the low-maturation kerogen matrices have more expandable interlayers and a higher content of aliphatic moieties, which should accommodate more PAH molecules, exhibiting greater overall sorption capacities. As the kerogen maturation increases, the content of the aliphatic domain decreases, and the aromatic interlayers become more rigid. The relative contribution of the aliphatic domain to the overall sorption decreases when compared to that of the aromatic domain. The relatively lower content of the aliphatic domain also lowers the overall sorption capacity for PAHs. When the kerogen matrix becomes highly matured and rigid, nonlinear adsorption on aromatic rigid backbones became dominant, and the overall sorption capacity is highly dependent on the surface properties of the kerogen samples. As shown previously [15], the specific surface area of LP7, XF7, and HZ7 is approximately 0.83, 17.1, and 29.7 m^3/g, respectively, which corresponds to an order of LP7 $<$ XF7 $<$ HZ7 for their respective single-point K_{OC} values calculated at a given C_e (Table 1).

The source material from which kerogen originates also may influence the sorption properties of the organic matrix. It is especially true for the low-maturation kerogen, because the relative contents of the flexible aliphatic domain are determined by the source materials [25]. For example, in the low-maturation XF samples, the dominant macerals are vitrinite, having abundant aliphatic chains [27], but even low-maturation HZ samples have macerals of fusinite and inertinite, in which the dominant carbon structures are more condensed aromatic sheets with short aliphatic side chains [28]. We can conclude from the above discussion that the XF sample exhibited greater contribution of the linear component, whereas the HZ sample exhibited more contribution of the nonlinear adsorption component to the overall sorption equilibria.

CONCLUSION

The present study indicated that kerogen materials having different source materials and different diagenetical histories exhibit very different sorption isotherm nonlinearity and capacity. The low-maturation kerogen matrices have high contents in the flexible aliphatic domain that exhibits nearly linear partitioning for sorption of PAHs, resulting in less nonlinear overall sorption with greater sorption capacity. As the kerogen matrix becomes more mature, the relative contents of the more rigid aromatic domain increase, and the site-limiting adsorption becomes dominant.

Kerogen particles found in soils and sediments may have very diverse chemical and structural properties because of the difference in the source materials and diagenetical and/or thermal histories. According to the present results, these soil/sediment-bound kerogen particles should not be treated as a single carbonaceous sorbent phase, and they may exhibit a wide range of sorption reactivities, with different isotherm nonlinearity and capacity. Accurate prediction of HOC sorption may require not only quantification of kerogen particles but also characterization of these particles in soils and sediments.

SUPPORTING INFORMATION

Fig. S1. The fitting of phenanthrene sorption data measured for lopinite (LP), lignite (XF), and fusinite (HZ) samples to the dual-mode model.

Fig. S2. The fitting of naphthalene sorption data measured for lopinite (LP), lignite (XF), and fusinite (HZ) samples to the dual-mode model.

All found at DOI: 10.1897/08-550.S1 (102 KB PDF).

Acknowledgement—The present study was funded by the Natural Science Foundation of China (40502031, 40573060) and the Natural Science Foundation of Guangdong Province (05300187). Partial funding also was provided by the Chinese Academy of Sciences, New Jersey Water Resource Research Institute, and Multistate Project (W-1082) from the U.S. Department of Agriculture Cooperative State Research, Education, and Extension Service to W. Huang.

REFERENCES

1. Song J, Peng P, Huang W. 2002. Black carbon and kerogen in soils and sediments. 1. Quantification and characterization. *Environ Sci Technol* 36:3960–3967.
2. Accardi-Dey A, Gschwend PM. 2002. Assessing the combined roles of natural organic matter and black carbon as sorbents in sediments. *Environ Sci Technol* 36:21–29.
3. Karapanagioti HK, Childs J, Sabaini D. 2001. Impacts of heterogeneous organic matter on phenanthrene sorption: Different soil and sediment samples. *Environ Sci Technol* 35:4684–4698.
4. Cornelissen G, Gustafsson Ö, Bucheli TD, Jonker MTO, Koelmans AA, van Noort PCM. 2005. Extensive sorption of organic compounds to black carbon, coal, and kerogen in sediments and soils: Mechanisms and consequences for distribution, bioaccumulation, and biodegradation. *Environ Sci Technol* 39:6881–6895.
5. Huang WL, Peng PA, Yu ZQ, Fu JM. 2003. Effects of organic matter heterogeneity on sorption and desorption of organic contaminants by soils and sediments. *Appl Geochem* 18:955–972.
6. Allen-King RM, Gratwohl P, Ball WP. 2002. New modeling paradigms for the sorption of hydrophobic organic chemicals to heterogeneous carbonaceous matter in soils, sediments, and rocks. *Adv Water Res* 25:985–1016.
7. Lohmann R, MacFarlane JK, Gschwend PM. 2005. Importance of black carbon to sorption of native PAHs, PCBs, and PCDDs in Boston and New York harbor sediments. *Environ Sci Technol* 39:141–148.
8. Ran Y, Xing BS, Rao PSC, Fu JM. 2004. Importance of adsorption (hole-filling) mechanism for hydrophobic organic contaminants on an aquifer kerogen isolate. *Environ Sci Technol* 38:4340–4348.
9. Bucheli TD, Gustafsson Ö. 2000. Quantification of the soot–water distribution coefficient of PAHs provides mechanistic basis for enhanced sorption observations. *Environ Sci Technol* 34:5144–5151.
10. Xiao BH, Yu ZQ, Huang WL, Song JZ, Peng PA. 2004. Black carbon and kerogen in soils and sediments. 2. Their roles in equilibrium sorption of less-polar organic pollutants. *Environ Sci Technol* 38:5842–5852.
11. Weber WJ, Huang WL, LeBoeuf EJ. 1999. Geosorbent and its relationship to the binding and sequestration of organic contaminants. *Colloids and Surfaces A: Physicochemical and Engineering Aspects* 151:167–179.
12. Xiao BH. 2004. The effects of soil organic matter heterogeneity on equilibrium sorption by soils and sediments. PhD thesis. Drexel University, Philadelphia, PA, USA.
13. Chiou CT, McGroddy SE, Kile DE. 1998. Partition characteristic polycyclic aromatic hydrocarbons on soils and sediments. *Environ Sci Technol* 32:264–269.
14. Ran Y, Xiao BH, Huang WL, Peng PA, Liu DH, Fu JM, Sheng GY. 2003. Effects of kerogen on the sorption of organic contaminants by a sandy aquifer material. *J Environ Qual* 32:1701–1709.
15. Yang C, Huang WL, Fu JM, Dang Z. 2009. Impact of kerogen heterogeneity on sorption of organic pollutants. 1. Sorbent characterization. *Environ Toxicol Chem* 28:1585–1591.
16. Cornelissen G, Gustafsson Ö. 2005. Importance of unburned coal carbon, black carbon, and amorphous organic carbon to phenanthrene sorption in sediments. *Environ Sci Technol* 39:764–769.
17. Weber WJ, Huang W. 1996. A distributed reactivity model for sorption by soils and sediments. 4. Intraparticle heterogeneity and phase-distribution relationships under nonequilibrium conditions. *Environ Sci Technol* 30:881–888.

18. Xing BS. 2001. Sorption of naphthalene and phenanthrene by soil humic acids. *Environ Pollut* 111:303–309.
19. Huang WL, Yu H, Weber WJ. 1998. Hysteresis in the sorption and desorption of hydrophobic organic contaminants by soils and sediments: 1. A comparative analysis of experimental protocols. *J Contam Hydrol* 31:129–148.
20. Wauchope RD, Koskinen WC. 1983. Adsorption–desorption equilibrium of herbicides in soil: A thermodynamic perspective. *Weed Sci* 31:504–512.
21. Huang WL, Weber WJ. 1997. A distributed reactivity model for sorption by soils and sediments. 10: Relationships between sorption, hysteresis, and the chemical characteristics of organic domains. *Environ Sci Technol* 31:2562–2569.
22. Perry RH, Chilton CH. 1973. *Chemical Engineer's Handbook.* McGraw-Hill, New York, NY, USA.
23. Xing B, Pignatello JJ, Gigliotti B. 1996. Competitive sorption between atrazine and other organic compounds in soils and model sorbents. *Environ Sci Technol* 30:2432–2440.
24. Durand B. 1980. *Kerogen: Insoluble Organic Matter from Sedimentary Rocks.* Technip, Paris, France.
25. Larsen JW, Kovac J. 1978. Organic chemistry of coal. *Am Chem Soc Symp Ser* 71:36–49.
26. Saxby JD, Bennett JR, Corcoran JF, Lambert DE, Riley KW. 1986. Petroleum generation: Simulation over six years of hydrocarbon formation from torbanite and brown coal in a subsiding basin. *Org Geochem* 9:69–81.
27. Liu DY, Peng PA. 2008. Possible chemical structures and biological precursors of different vitrinites in coal measure in northwest China. *Int J Coal Geol* 75:204–212.
28. Sun XG. 2005. The investigation of chemical structure of coal macerals via transmitted-light FT-IR microspectroscopy. *Spectrochim Acta A Mol Biomol Spectrosc* 62:557–564.